EUROPEAN ORGANIZATION FOR NUCLEAR RESEARCH

CERN-EP/82-20
19 February 1982

EVIDENCE OF A RISE IN THE ANTIPROTON-PROTON TOTAL CROSS-SECTION AT THE CERN INTERSECTING STORAGE RINGS

G. Carboni*) and D. Lloyd Owen

CERN, Geneva, Switzerland

M. Ambrosio, G. Anzivino, G. Barbarino, G. Paternoster and S. Patricelli

Istituto di Fisica dell'Università, Napoli, and INFN, Sezione di Napoli, Italy

V. Cavasinni**), T. Del Prete, M. Morganti and M. Valdata-Nappi

INFN, Sezione di Pisa and Istituto di Fisica dell'Università, Pisa, Italy

P.D. Grannis

State University of New York, Stony Brook, USA

ABSTRACT

We measured the total cross-section for $\bar{p}p$ scattering at $\sqrt{s}$ = 52.8 GeV at the CERN ISR, using the direct, total-rate method. The result obtained, $\sigma_{tot}(\bar{p}p)$ = = 44.70 ± 0.53 mb, shows that, in common with $\sigma_{tot}(pp)$, this cross-section also starts to rise in the ISR energy range. We remeasured the total cross-section for pp scattering at the same energy, obtaining $\sigma_{tot}(pp)$ = 43.26 ± 0.33 mb, and found for the difference, $\Delta\sigma_{tot} = \sigma_{tot}(\bar{p}p) - \sigma_{tot}(pp)$, a value of 1.44 ± 0.45 mb.

(Submitted to Physics Letters B)

---

*) On leave of absence from INFN, Sezione di Pisa, Italy.

**) Also at Istituto di Fisica dell'Università, Bologna, Italy.

Since the introduction of antiprotons into the CERN ISR in April 1981, the CERN-Napoli-Pisa-Stony Brook experiment has been installed in Intersection Region 2 with a set of detectors covering virtually the entire solid angle. The primary aims of the experiment are the measurement of the total cross-sections for $\bar{p}p$ and pp collisions via the observation of the total interaction rates, the measurement of the differential cross-sections for small-angle elastic scattering, and a comparative study of the general features of multiparticle production through measurements of multiplicity and pseudorapidity distributions. The determination of σ_{tot} in this experiment is quite direct: the observed collision rate is 94% of the total interaction rate and so only small corrections are required.

Preliminary results obtained during early $\bar{p}p$ runs have already been reported [1,2]; however, poor statistics due to the lowness of the machine luminosity was not sufficient to establish unambiguously the rise of the $\bar{p}p$ cross-section in the ISR energy range. The results reported in this letter come from a 14-day run in October 1981, in which a stochastically cooled $\bar{p}$ beam was in circulation with a current of 2mA. This beam collided with a p beam of about 10 A, giving a luminosity of approximately 7×10^{26} cm^{-2} s^{-1}. The mean centre-of-mass energy was $\sqrt{s}$ = 52.8 GeV. Proton-proton data were also collected for comparison (mainly with equal currents in both beams), and both sets of data were analysed in the same way.

The experimental arrangement is indicated in fig. 1; the apparatus has left-right symmetry with respect to the beam crossing. Both the left arm and the right arm consist of five sets of hodoscopes spanning the polar region $0.2^\circ < \theta \leq 90^\circ$ in successive steps. Each set of hodoscopes comprised two planes of trigger counters operated in coincidence and a further plane of small counters used to localize particle hits in θ and ϕ. In addition, a drift-chamber hodoscope was sandwiched between the CI and CO hodoscopes. The drift chambers were mainly used to study multiplicities in the polar range $|\eta| < 2$, but in the results presented here they were used to establish the event vertex for certain classes of events thus discriminating against background. Finally, the TB hodoscope was also equipped with two planes of drift tubes, which served to determine the slopes of the differential elastic cross-sections needed to estimate a small correction term for elastic losses.

The trigger for the experiment was the requirement of a coincidence of hits in the left and right arms. A hit in either arm was signalled by the sum of the coincidences between overlapping elements in each hodoscope set:

$$\mathrm{Hit}_{L,R} = (\mathrm{CI}\cdot\mathrm{CO} + \mathrm{H}_1\cdot\mathrm{H}_2 + \mathrm{H}_3\cdot\mathrm{H}_4 + \mathrm{H}_{5A}\cdot\mathrm{H}_{5B} + \mathrm{TB}_A\cdot\mathrm{TB}_B)_{L,R} .$$

For each trigger, the presence of hits in all cells of all hodoscopes was encoded and recorded. The time difference between a master pulse and each coincidence in the trigger was also recorded.

In the off-line analysis, we formed the time difference between the signals from each left-arm hodoscope set and the signals from each right-arm hodoscope set. Twenty-five left-right time differences, t_i, could thus be constructed if all hodoscopes in the experiment were struck in a particular event. In practice, most interactions resulted in hits in a majority of the hodoscopes, so the timing information was highly redundant.

From pp data, the mean time difference $\langle t_i \rangle$, characterizing beam-beam events for each left-right combination i, was obtained and also the FWHM Γ_i of each distribution ($\simeq$ 6 ns). Triggers resulting from the upstream interactions of either beam with the gas in the vacuum pipe or the pipe itself had a time-ordered sequence of hodoscope hits as the secondaries swept through the apparatus from left to right (or vice versa), resulting in t_i values that differed from the $\langle t_i \rangle$ values in proportion to the physical separation of the hodoscopes involved.

From the available timing information we formed the quantity

$$T^2 = \frac{1}{N_{td}} \sum_{i=1}^{N_{td}} \frac{(t_i - \langle t_i \rangle)^2}{\Gamma_i^2}$$

to test the hypothesis that an event arose from the beam-crossing region (N_{td} denotes the number of time differences observed for the event).

The distribution of events in T^2 is shown in fig. 2 for both $\bar{p}p$ and pp runs. The pp run shows virtually no events with $T^2 > 2$, in accordance with the negligible

contamination from single-beam background. For the $\bar{p}p$ run, in addition to the low-T^2 peak seen in pp, there is a broad peak centred at $T^2 = 5$ consisting of single-beam events. The events with $T^2 < 2$ formed our candidate beam-beam sample; those with $T^2 > 2$ were used to monitor the amount of background contaminating this sample.

In $\bar{p}p$ runs, single-beam background was particularly troublesome for the subset of events in which the only hit on the right was $CI \cdot CO_R$, since time differences involving this hodoscope did not discriminate well between beam-beam and single-beam events. The beam-beam content of this set of events was small ($\simeq 0.5\%$ of the total beam-beam rate) and was overwhelmed by background events from the proton beam. Consequently, a partial rate R_1 was computed neglecting this set of events. Events in which the only hit on the left was in the central box, i.e. the triggers $(CI \cdot CO)_L \cdot (H_1 \cdot H_2 + H_3 \cdot H_4 + H5_A \cdot H5_B + TB_A \cdot TB_B)_R$, did not present the same problem because of the asymmetry of the background. The rate R_2 of the latter events was obtained separately. Because of the symmetry of the apparatus and of the reaction R_2 is also the rate lost because of the exclusion of the events $(H_1 \cdot H_2 + H_3 \cdot H_4 + H5_A \cdot H5_B + TB_A \cdot TB_B)_L \cdot (CI \cdot CO)_R$ from the initial sample*). Finally, the rate R_3 of the events firing the central detector only had to be taken into account. For pp interactions, R_3 was determined directly since the contamination from single-beam background was so small: 0.025% of the observed beam-beam rate triggered only $(CI \cdot CO)_L \cdot (CI \cdot CO)_R$. In the $\bar{p}p$ case, we discriminated between beam-beam and single-beam events by reconstructing the event vertex with the central chambers. The central-hodoscope contribution to the $\bar{p}p$ cross-section determined in this manner was found to be of the same order as in the pp case.

The total observed rate was thus defined as

$$R_{obs} = R_1(T^2 < 2) + R_2(T^2 < 2) + R_3(T^2 < 2).$$

As can be seen from figs. 2b and 2c, a relatively large amount of background still survived at $T^2 < 2$, affecting R_{obs} particularly in the low-luminosity $\bar{p}p$ runs.

---

*) The left-right symmetry of the apparatus was checked to a precision of 0.1% during pp runs.

To separate the beam-beam signal from this background, we used the method [3] of varying the machine luminosity L.

At each luminosity, the measured rate R_{obs} consists of the beam-beam interaction rate, σ_{obs} L, and a rate of background events:

$$R_{obs} = \sigma_{obs} L + R_B . \quad (1)$$

The rate R_B was found to be proportional to the rate of events having $T^2 > 2$, so that eq. (1) could be rewritten:

$$R_{obs} = \sigma_{obs} L + \beta R (T^2 > 2) . \quad (2)$$

By repeating the meaurement at different values of L, β and σ_{obs} were obtained by fitting eq. (2) to the data. The method was very insensitive to the background, provided that $|\Delta R_B| \ll \sigma_{obs} |\Delta L|$: typically, L was varied by a factor of 10^3, while the background changed by less than 10%. The required variation in the luminosity was achieved by displacing the beams vertically so as to change their overlap. In practice, pp data were taken during special calibration runs, when the machine luminosity was measured by the Van der Meer method [1,4]. The $\bar{p}p$ data were collected with the beams at full overlap (signal runs) and with the $\bar{p}$ beam displaced 4 mm vertically so that no beam-beam interactions occurred (background runs). The p beam was not moved to avoid influencing the background. Many such pairs of runs were taken and their duration ($\sim \frac{1}{2}$ hour) was kept much shorter than the time scale of background evolution.

The luminosity was obtained using a system of monitor coincidences which were chosen with particular care to be sensitive only to beam-beam interactions. For $\bar{p}p$ runs, the monitor

$$M_1 = (H_3 \cdot H_4)_L \cdot (H_{5_A} \cdot H_{5_B})_R$$

satisfied this requirement. In the case of pp runs, we took advantage of the much cleaner conditions to use the entire apparatus as a monitor:

$$M_2 = Hit_L \cdot Hit_R .$$

The monitor rate R_{mon} yielded the luminosity directly:

$$L = \frac{R_{mon}}{\sigma_{mon}} ,$$

where σ_{mon} denotes the inclusive cross-section for events triggering the monitor. (In the case of the monitor M_2, σ_{mon} was just the observed cross-section σ_{obs}). This parameter was measured repeatedly by the Van der Meer method [1,4] in special runs interleaved with the data taking.

During pp calibration runs, σ_{M_2} was also obtained, in order to check the reproducibility of this monitor. The results from several runs are shown in table 1. The pp data were taken over a large range of beam currents, as a check against potential rate effects, and one measurement was made with unbalanced currents (10 A vs. 5 mA) to simulate conditions encountered during $\bar{p}p$ running. As table 1 shows, high and low luminosity values agree to within 0.5%, the intrinsic precision of the Van der Meer method.

For both the $\bar{p}p$ and the pp reaction, the observed cross-sections had to be corrected for two sources of loss:

i) elastic events where one or both of the elastically scattered particles did not emerge from the vacuum chamber, and

ii) single-diffractive events where the quasi-elastically scattered particle remained in the vacuum chamber.

Elastic scattering was measured in special runs using the small-angle TB hodoscopes. In the analysis, we demanded a collinear pattern of left and right TB hits with no evidence of extra particle production in the large-angle hodoscopes. The distribution in t of elastic events was obtained in the region $0.01 < |t| < 0.05$ GeV^2 and the exponential slope extrapolated to $|t| = 0$. Integrating over the region of the holes in the detector ($|t| < 0.06$ GeV^2), we obtained the elastic correction $\Delta\sigma_{el}$.

The inelastic loss $\Delta\sigma_{inel}$ was obtained by a similar extrapolation. We selected a sample of events in which there was a hit with $\theta > 40$ mrad in one arm, thus

excluding elastic events. The collection of hits in the opposite arm was then examined and the hit of largest angle, θ_{max}, found. The distribution of these events was obtained as a function of $t' = (p\theta_{max})^2$, where p is the beam momentum. The small-t' behaviour was found to be exponential with a slope of about half that for elastic scattering. Extrapolating and integrating the distribution, we were able to predict the magnitude of this loss in a straightforward manner.

The size of the small-angle corrections was not sensitive to the values of the slope parameters used in the extrapolations: in the elastic case the $|t| = 0$ intercept was fixed by the optical theorem; in the inelastic case the slope was relatively small.

The final results, $\sigma_{tot}(\bar{p}p)$ and $\sigma_{tot}(pp)$, are listed in table 2 along with the values of the observed cross-sections and the increments used to correct for losses. The relatively large errors in the small-angle correction terms are due to imperfect knowledge of the geometry of the TB hodoscopes. These cancel to first order when $\bar{p}p$ and pp results are compared, so we regard $\Delta\sigma = 1.44 \pm 0.45$ mb as the most reliable determination of $\sigma_{tot}(\bar{p}p) - \sigma_{tot}(pp)$.

In fig. 3 our cross-sections are compared with earlier results over a broad energy range. The value we found for $\sigma_{tot}(pp)$, 43.26 ± 0.33 mb, is slightly higher than the currently accepted value at $\sqrt{s} = 52.8$ GeV [5]. Our result would be in better agreement with earlier ones but for the recent discovery that the vertical-beam-displacement scale at the ISR is $(2.0 \pm 0.2)\%$ higher than the nominal one at 26 GeV/c momentum [6]. This discrepancy results in an overestimate in the luminosity if the nominal displacements are used, but whether the same correction is necessary for pre-1981 data is not clear.

We compare our value for the $\bar{p}p$ total cross-section at $\sqrt{s} = 52.8$ GeV, $\sigma_{tot}(\bar{p}p) = 44.70 \pm 0.53$ mb, with the value found at $\sqrt{s} = 19.4$ GeV, $\sigma_{tot}(\bar{p}p) = 41.44 \pm 0.18$ mb [7]: our result is higher by 3.26 ± 0.56 mb, showing conclusively that, as expected [8,9], the $\bar{p}p$ total cross-section rises in the ISR energy range.

In closing, we should like to thank the staff of the Proton Synchrotron Division, of the Antiproton Accumulator Group, and especially of the Intersecting Storage Rings Division, for the remarkable achievement that has made this measurement possible. We are particularly grateful to G. Kantardjian and K. Potter for their close collaboration throughout all stages of the experiment. We also wish to thank E. Gabathuler and A. Wetherell for their continuous interest in and support of the experiment. The technical support of G. Barnini, A. Donnini, L. Giacomelli, T. Regan, and the technical staff of the University of Naples is gratefully acknowledged.

REFERENCES

[1] G. Carboni et al., Phys. Lett. 108B (1982) 145.

[2] D. Favart et al., Phys. Rev. Lett. 47 (1981) 1191.

[3] L. Baksay et al., Nucl. Phys. B141 (1978) 1.

[4] S. Van der Meer, CERN Internal Report ISR-OP/68-31 (1968).

[5] U. Amaldi and K.R. Schubert, Nucl. Phys. B166 (1980) 301.

[6] K. Potter, ISR performance report, November 1981.

[7] A.S. Carroll et al., Phys. Lett. 61B (1976) 303.

[8] U. Amaldi et al., Phys. Lett. 66B (1977) 390.

[9] H.J. Lipkin, Phys. Rev. D 17 (1979) 366.

Table 1

Monitor cross-sections[a)]

Luminosity run	Reaction type	I_1 (A)	I_2 (A)	σ_{M_1} (mb)	σ_{M_2} (mb)
1	pp	10.4	10.3	11.77 ± 0.05	40.84 ± 0.09
2	pp	10.4	5.10×10^{-3}	11.60 ± 0.13	-
3	pp	2.15	2.22	11.63 ± 0.06	40.78 ± 0.11
4	pp	2.15	2.22	11.64 ± 0.06	40.76 ± 0.11
5	pp	3.46	3.52	11.60 ± 0.04	40.70 ± 0.07
6	pp	3.46	3.52	11.55 ± 0.04	40.59 ± 0.07
7	pp	3.46	3.52	11.57 ± 0.04	40.62 ± 0.07
8	pp	1.04	1.02	11.69 ± 0.05	-
9	$\bar{p}p$	10.3	1.99×10^{-3}	12.29 ± 0.12	-
10	$\bar{p}p$	6.4	1.95×10^{-3}	12.36 ± 0.14	-
11	$\bar{p}p$	8.9	1.88×10^{-3}	12.32 ± 0.09	-

a) Errors given are statistical only.

Table 2

Summary of results on the total cross-sections[a] at $\sqrt{s}$ = 52.8 GeV

Reaction type	Integrated luminosity (cm^{-2})	σ_1[b] (mb)	σ_2[b] (mb)	σ_3[b] (mb)	σ_{obs} (mb)	$\Delta\sigma_{el}$ (mb)	$\Delta\sigma_{inel}$ (mb)	σ_{tot} (mb)
$\bar{p}p$	1×10^{31}	41.84 ± 0.40	0.25 ± 0.02	0.04 ± 0.02	42.13 ± 0.40	2.05 ± 0.10	0.52 ± 0.03	44.70 ± 0.40 ± 0.13
pp	5×10^{31}	40.50 ± 0.20	0.24 ± 0.02	0.01 ± 0.001	40.75 ± 0.20	2.00 ± 0.10	0.51 ± 0.03	43.26 ± 0.20 ± 0.13

a) The errors on σ_1, σ_2, and σ_3 are purely statistical and include a ± 0.5% error on the luminosity calibration. The errors on the correction terms, $\Delta\sigma_{el}$ and $\Delta\sigma_{inel}$, are mainly systematic and are the same for both reactions.

b) σ_1, σ_2, and σ_3 are the partial cross-sections corresponding to the partial beam-beam rates, R_1, R_2, and R_3, discussed in the text. $\sigma_{obs} = \sigma_1 + \sigma_2 + \sigma_3$.

Figure captions

Fig. 1 : Schematic layout of the apparatus: CI, CO, H_1, H_2, H_3, H_4, H_5, and TB are scintillation counter hodoscopes. H_5 and TB have each two trigger planes (A, B) in coincidence to provide the trigger signal. The dotted lines represent the finely-divided hodoscope planes used to measure the direction of charged secondaries. In this work they were used to provide data for the small-angle extrapolations. DC is a drift-chamber vertex detector.

Fig. 2 : Distribution of the events versus T^2: a) pp run; b) $\bar{p}p$ run, beams at full overlap; c) $\bar{p}p$ run, beams separated 4 mm vertically. The region $T^2 < 2$ mainly contains beam-beam events. The residual peak at $T^2 < 2$ in (c) is due to single-beam events hitting the beam pipe near the beam-crossing point. The beam-gas background at $T^2 > 2$ is almost negligible in case (a) owing to the higher luminosity attained in pp stacks compared with $\bar{p}p$ stacks.

Fig. 3 : Dependence of the total cross-section, $\sigma_{tot}(pp)$ and $\sigma_{tot}(\bar{p}p)$, on the c.m. energy. Fermilab data are from ref. 7. Previous ISR data are from the compilation in ref. 5.

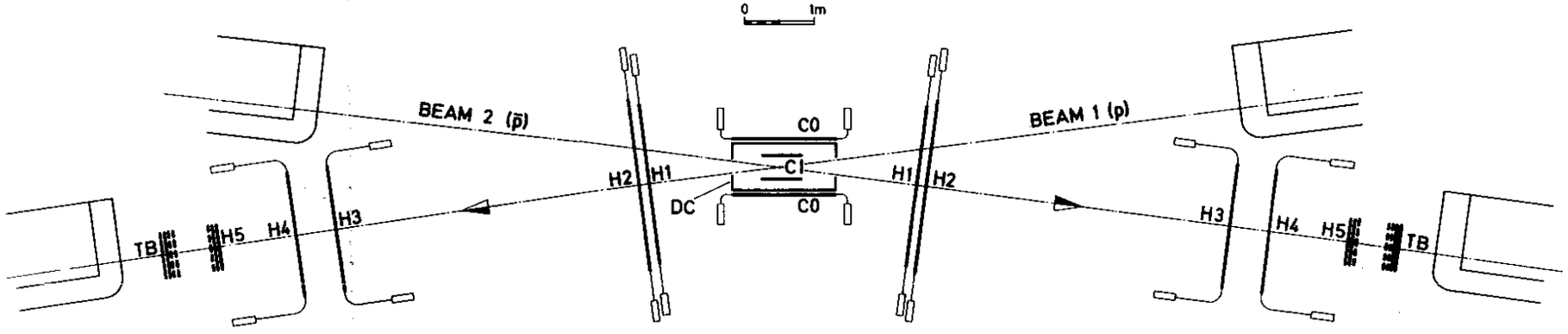
0
1m
BEAM 2 (p̄)
BEAM 1 (p)
C0
C1
C0
DC
H1
H2
H2
H1
H3
H4
H5
TB
H3
H4
H5
TB
LEFT
RIGHT

Fig. 1

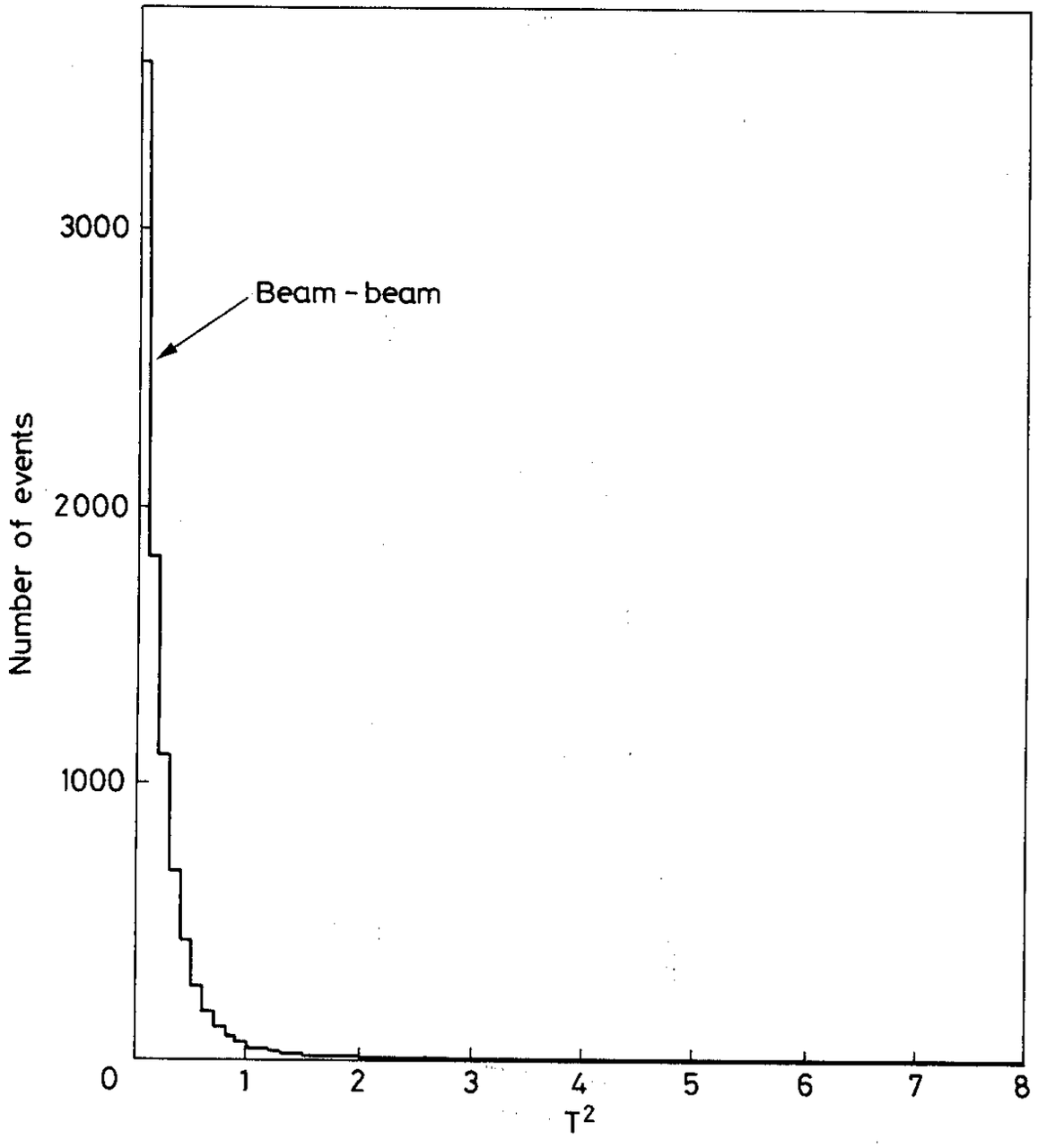

Fig. 2a

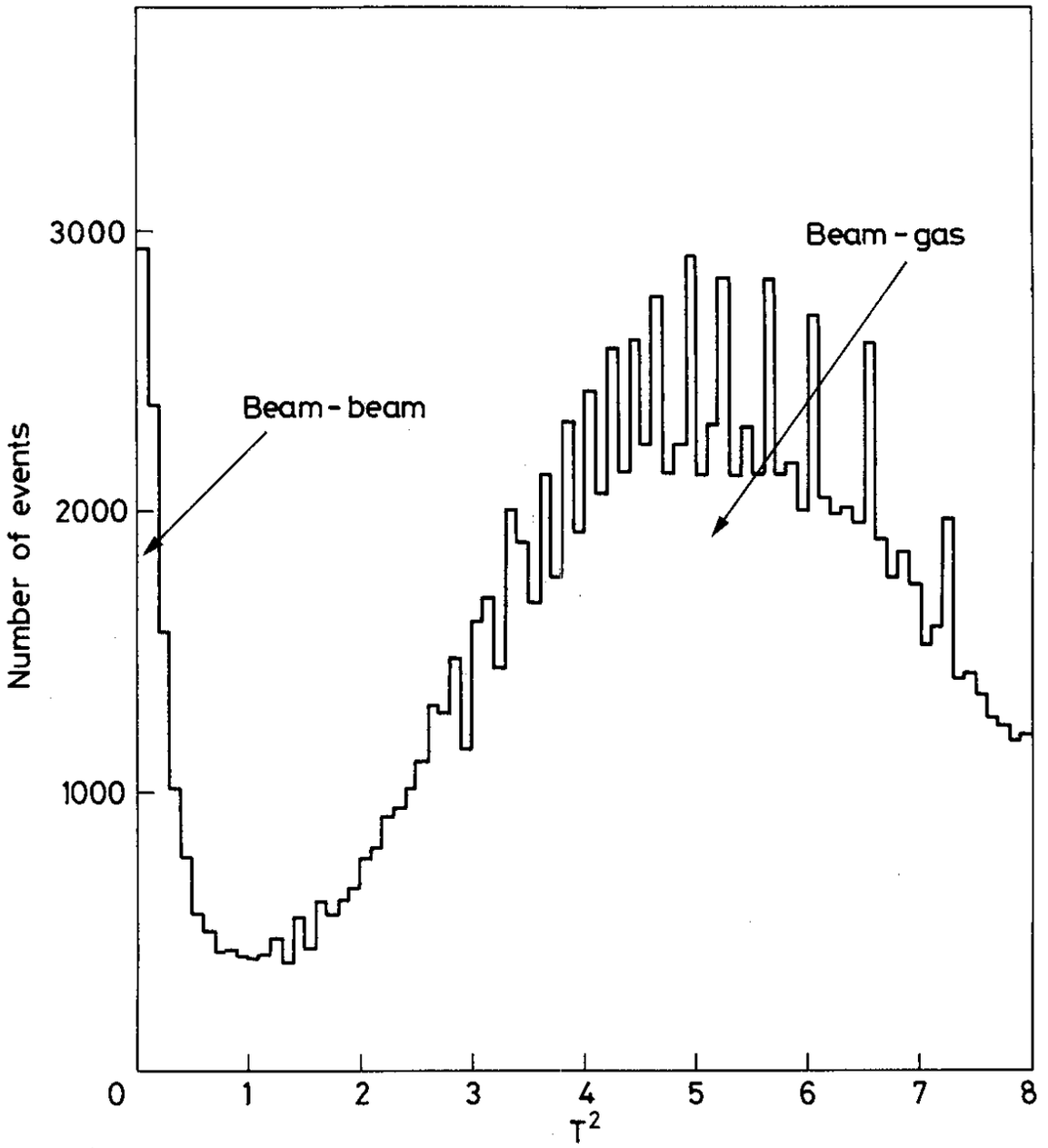
3000
2000
1000
0
Number of events
Beam - beam
Beam - gas
1
2
3
4
5
6
7
8
T^2

Fig. 2b

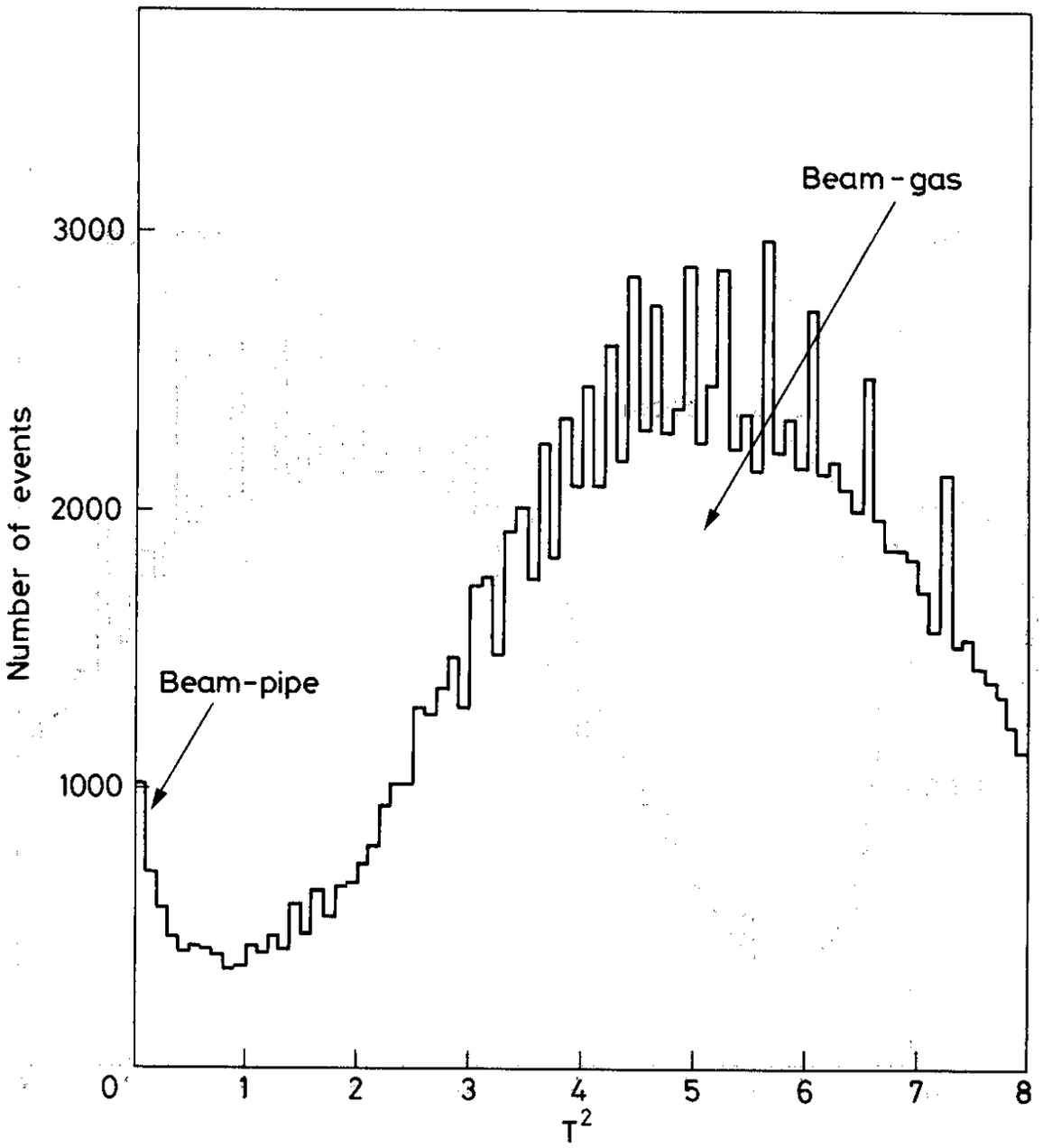
Beam-gas
Beam-pipe
Number of events
3000
2000
1000
0
1
2
3
4
5
6
7
8
T^2

Fig. 2c

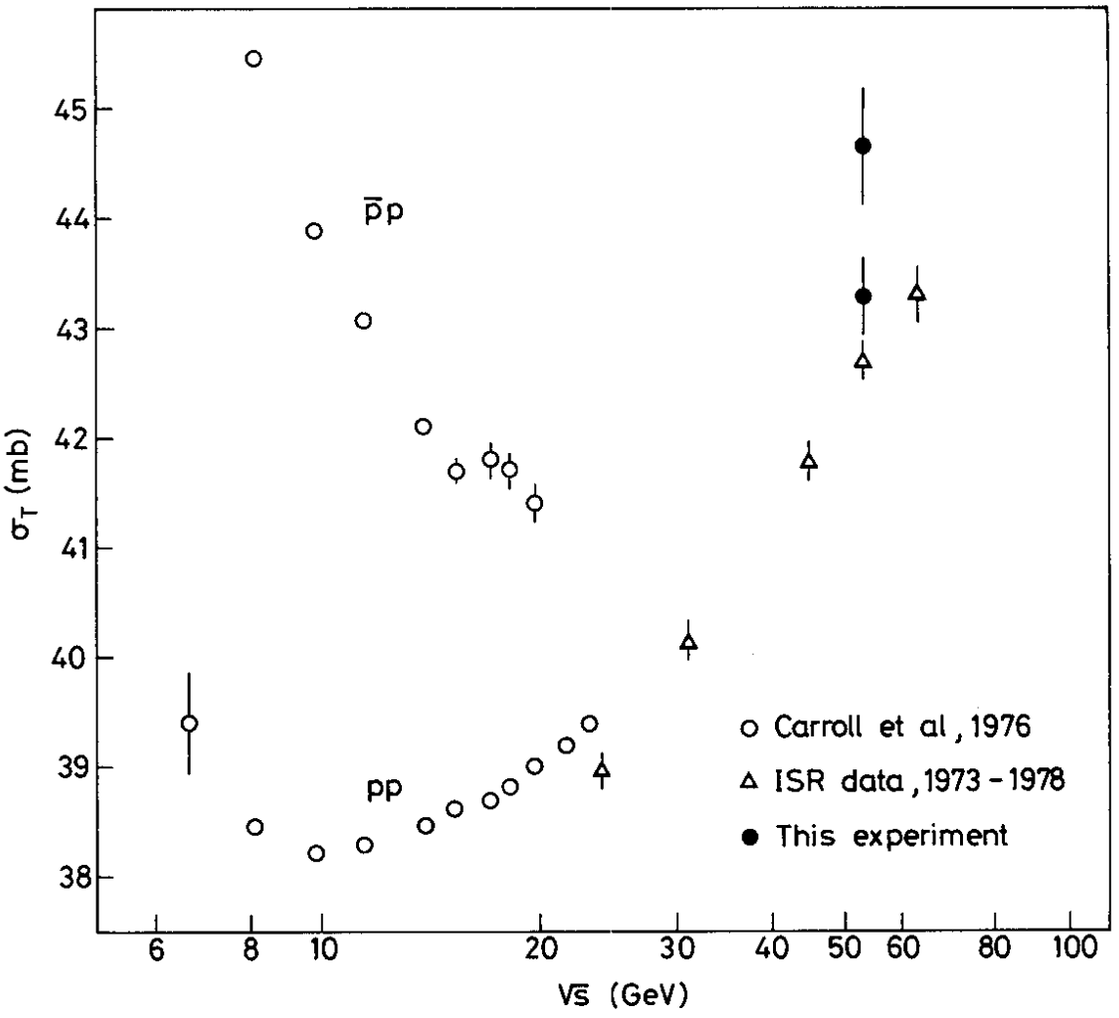
45
44
43
42
41
40
39
38
σ_T (mb)
$\bar{p}p$
pp
Carroll et al, 1976
ISR data, 1973 - 1978
This experiment
6
8
10
20
30
40
50
60
80
100
$\sqrt{s}$ (GeV)

Fig. 3